Journal of Chromatography B, 876 (2008) 47–53

Contents lists available at ScienceDirect

Journal of Chromatography B

journal homepage: www.elsevier.com/locate/chromb

Characterization of the *in vivo* and *in vitro* metabolic profile of PAC-1 using liquid chromatography–mass spectrometry

Lei Ren[a], Kaishun Bi[a], Ping Gong[b], Weiming Cheng[a], Zhen Song[a], Lina Fang[a], Xiaohui Chen[a,*]

[a] School of Pharmacy, Shenyang Pharmaceutical University, 103 Wenhua Road, Shenyang 110016, China
[b] School of Pharmaceutical Engineering, Shenyang Pharmaceutical University, 103 Wenhua Road, Shenyang 110016, China

ARTICLE INFO

Article history:
Received 30 July 2008
Accepted 7 October 2008
Available online 14 October 2008

Keywords:
Metabolite identification
PAC-1
TOF/MS
Ion trap

ABSTRACT

In the present study, the metabolic profile of PAC-1, a potential anticancer drug, was investigated using liquid chromatography–mass spectrometric (LC/MS) techniques. Two different types of mass spectrometers – a quadrupole time-of-flight (Q-TOF) mass spectrometer and an ion trap (IT) mass spectrometer – were employed to acquire structural information on PAC-1 metabolites. A gradient liquid chromatographic system composed of 0.2% formic acid in methanol and 0.2% formic acid in water was used for metabolite separation on an Agilent TC-C_{18} column. A total of 16 metabolites were detected. The corresponding product ion spectra were acquired and interpreted, and structures were proposed. Accurate mass measurement using LC-Q-TOF was used to determine the elemental composition of metabolites thereby confirming the proposed structures of these metabolites. Phase I metabolic changes were predominantly observed, including debenzylation, dihydrodiol formation, hydroxylation, and dihydroxylation. The detected phase II metabolites included PAC-1 and hydroxylated PAC-1 glucuronide conjugates. Based on metabolite analysis, several PAC-1 metabolic pathways in rat were proposed.

1. Introduction

Drug discovery and development is a long and expensive process, in which metabolite identification of new chemical entities (NCEs) at various different stages of the process is required. In the past, metabolite identification occurred generally only after a drug candidate was selected for development. However, drug metabolism can dramatically influence a drug's distribution, rate or route of excretion, and rate of production of new and possibly toxic species. Currently, drug metabolism studies are used to optimize drug candidates, and are required before a NCE can advance toward development and market [1–3].

PAC-1, (4-benzyl-piperazin-1-yl)-acetic acid (3-allyl-2-hydroxy-benzylidene)-hydrazine, is among the small anti-cancer agents, discovered by Putt et al. [4]. Early biochemical studies showed that PAC-1 directly activates procaspase-3 to caspase-3, an anticancer strategy that may prove beneficial in treating a wide variety of cancers [4]. As a target compound, PAC-1 has attracted significant attention since it is active both *in vitro* and *in vivo* against mice tumors. However, the mechanism of action remains an area of debate, specifically as to whether PAC-1 directly or indirectly activates procaspase-3 to caspase-3 [5–9]. To understand and design more potent compounds that have better pharmacodynamic (PD) and pharmacokinetic (PK) properties, there is a demand to more fully understand the drug metabolism and pharmacokinetics (DMPK) characteristics of PAC-1.

Previously in our group, the PK properties of PAC-1 after intravenous and oral administration in rat were studied with HPLC. The oral bioavailability (%F) of PAC-1 was 23% at 50 mg/kg in rats, a value that may be due, in part, to hepatic and intestinal first-pass effects (submitted for publication). While metabolic data are important to optimize a drug candidate, metabolic pathways of PAC-1 *in vitro* and *in vivo* have not yet been reported, to the best of our knowledge.

Highly selective and sensitive liquid chromatography coupled with mass spectrometry (LC/MS) is a powerful technique for the identification of drug metabolites in biological matrices [10–13]. Among several different LC/MS platforms, Q-TOF/MS is especially helpful for the identification of drug metabolites as it can provide elemental composition from accurate mass measurement. Thus, metabolite structures can be proposed with high degrees of certainty without the need of standards for each metabolite [14].

In the present study, experiments were conducted for mass spectral qualitative structural elucidation of the predominant

* Corresponding author. Tel.: +86 24 23986259 fax: +86 24 23986259.
E-mail address: cxh_syphu@yahoo.com.cn (X. Chen).

1570-0232/$ – see front matter.
doi:10.1016/j.jchromb.2008.10.006

metabolites of PAC-1 *in vivo* and *in vitro* using LC-Q-TOF/MS and LC-ITMS.

2. Experimental

2.1. Chemicals and reagents

PAC-1 (>98% pure) was purchased from Sigma Chemical Co. (St. Louis, MO, USA), and des-benzyl-PAC-1 (>98% pure based on UV analysis) was prepared in our laboratory. Their structures were confirmed by positive ESI-MS^n and ^1H NMR. NADPH was purchased from Roche (Basel, Switzerland). Tris-(hydroxymethyl) aminomethane (ultra pure grade) was purchased from ANGUS (Illinois, USA). HPLC grade methanol was purchased from Tedia Co., Inc. (Fairfield, USA). HPLC grade formic acid was purchased from Kermel Chemical Reagent Co., Ltd. (Tianjin, China). Distilled water, prepared with demineralized water, was used throughout the study.

2.2. Instrumentation

LC-Q-TOF/MS experiments were performed on a Bruker Daltonics micrOTOF-Q mass spectrometer (Billerica, MA, USA) with an Agilent 1200 HPLC. The software micrOTOF control (Version 2.2) was applied for system operation and data collection. LC-MS^n experiments were carried out on an Agilent LC/MSD Trap SL (Agilent Technologies, Waldbronn, Germany) with an Agilent 1100 HPLC. All data acquired were processed by Agilent LC/MSD Trap software 5.3 (Agilent, Palo Alto, CA, USA). Both mass spectrometers were equipped with electrospray ionization (ESI) source and operated in positive ion mode. A high speed desk centrifuge (TGL-16C, Shanghai Anting Scientific Instrument Factory, Shanghai, China) was used for all sampled centrifugation.

2.3. Chromatographic conditions

Both the Agilent 1200 HPLC for Q-TOF/MS and Agilent 1100 HPLC for ITMS were equipped with a reversed phase column (Agilent TC-C_{18}, 150 mm × 4.6 mm i.d., 5 μm, USA) protected by a 4.0 mm × 3.0 mm i.d. security guard (5 μm) C_{18} guard column (Phenomenex, Torrance, CA, USA). The mobile phase of a gradient mixture of A (0.2% formic acid in methanol) and B (0.2% formic acid in water) programmed according to the following protocol: initial 40% A maintained for 3 min, then increased to 60% in 7 min; maintained at 60% for 5 min and finally decreased to 40% A in 1 min, then maintained at 40% for 4 min. The flow rate was 0.6 mL/min with an injection volume of 20 μL.

2.4. Mass spectrometric conditions

For all LC-Q-TOF/MS experiment, the capillary voltage of the ion source was set at 4500 V and the capillary exit was set at 90 V. Hexapole radio frequencies 1 and 2 were set to 200 Vpp and 300 Vpp, respectively. Nitrogen was used as the desolvation and nebulizing gas at a constant temperature of 190 °C. For CID experiments, argon was used as the collision gas and the collision energy was set to 20 eV. The scan range was set at *m/z* 100 – 1000. Instrument calibration was performed with a sodium formate solution consisting of 10 mM sodium hydroxide in isopropanol/0.2% formic acid (1:1, v/v). The theoretical exact masses of the calibration ions were 158.9641, 226.9515, 294.9389, 362.9263, 430.9138, and 498.9012, corresponding to the formulas $Na(NaCOOH)_2$, $Na(NaCOOH)_3$, $Na(NaCOOH)_4$, $Na(NaCOOH)_5$, $Na(NaCOOH)_6$ and $Na(NaCOOH)_7$, respectively. Automated post-run internal mass scale calibration of individual samples was performed by injecting the calibrant at the beginning of each run *via* a six-port divert valve equipped with a 100 μL loop.

For LC-ITMS experiments, the interface and MSD parameters were set according to the following protocol: nebulizer pressure 30 psi (N_2), drying gas 8 L/min (N_2), dry gas temperature 325 °C, spray capillary voltage 4.0 kV, skimmer voltage 40 V, ion transfer capillary exit 128 V, scan range *m/z* 50–800, spectra average 5, target 30,000, and rolling average 2. For MS^n spectra, the fragmentation amplitude varied between 0.7 V and 0.9 V. The MS^n product-ion spectra were produced by collision induced dissociation (CID) of the molecular ion $[M+H]^+$ of all analytes at their respective HPLC retention times. Data acquisition was performed in full-scan LC-MS and MS^n modes.

2.5. Sample preparation

Three groups of six male Wistar rats (200 g ± 20 g in weight) were provided by the Experimental Animal Center of Shenyang Pharmaceutical University. Animal experiments were conducted in accordance with the Guidelines for Animal Experimentation of Shenyang Pharmaceutical University (Shenyang, China) and all procedures were approved by the Animal Ethics Committee of this institute. Animals were fasted for 12 h with free access to water prior to each experiment.

2.5.1. In vivo samples

Feces and urine samples were collected within a period of 0–24 h after administration of a single 50 mg/kg oral dose of PAC-1. After drugs were administered, rats were fixed in a Bollman cage. Bile was collected in a micro-tube via a polyethylene tube inserted into the bile duct within a period of 0–24 h. Drug-free rat urine, feces, and bile were also collected prior to dosing. All the samples were stored at −20 °C until analysis.

A 100 mg aliquot of feces was weighted in a glass tube, and 1 mL methanol and 1 mL water were added. The mixture was sonicated for 10 min, and then centrifuged for 10 min at 4000× *g*. A 0.5 mL aliquot of the supernatant layer was transferred to a glass tube and extracted for 5 min with 3 mL ethyl acetate. After centrifugation (4000× *g*, 5 min), the organic phase was transferred to another vial and evaporated to dryness in a thermostatically-controlled water bath at 37 °C under a slight stream of nitrogen. The residue was then dissolved in 100 μL methanol and water (40:60, v/v), and a 20 μL aliquot of the supernatant was used for identification of metabolites.

To a 200 μL aliquot of urine or bile sample, 400 μL methanol was added. This mixture was vortexed and centrifuged at 16,000× *g* for 5 min. The supernatant was transferred to a glass tube, evaporated to dryness under a stream of nitrogen, and then reconstituted in 100 μL methanol and water (40:60, v/v). A 20 μL aliquot of supernatant was used for identification of metabolites.

2.5.2. In vitro samples

Rat liver microsomes (RLM) were prepared according to a previously described method [15]. Microsomal protein concentrations were measured according to the procedure of Markwell et al. using bovine serum albumin (BSA) as a standard [16]. Enzyme-activity was measured according the procedure of Omura and Sato [17].

In all experiments, PAC-1 was dissolved in methanol and NADPH was dissolved in tris (hydroxymethyl) aminomethane hydrochloride-potassium chloride (Tris–HCl–KCl) solutions. For microsomal metabolism of PAC-1, the final volume of the incubation mixture was 500 μL, which consisted of 50 μM PAC-1 and 1 mg of microsomal protein/mL, at pH 7.4. The final concentration of the organic solvent did not exceed 1%. Metabolism was initiated

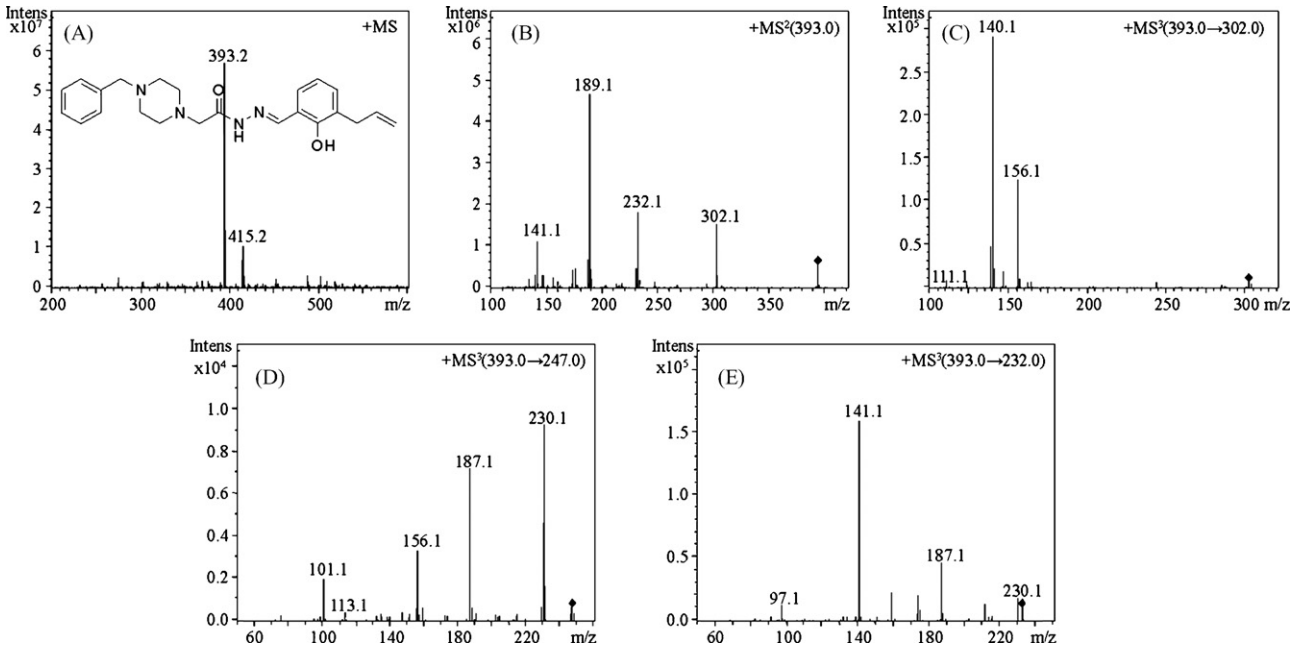

Fig. 1. MS (A), MS/MS (B) and MS^3 (C), (D) and (E) spectra of PAC-1 under positive ESI source.

by the addition of NADPH (1 mM) after preincubation of microsomal incubates at 37 °C for 3 min, and this incubation was continued for 60 min in a shaking water bath. Control incubations were conducted with heat-denatured microsomal preparations (80 °C for 10 min). The reaction was quenched by adding 500 μL ice-cold acetonitrile and the contents were vortex mixed for 3 min, and then centrifuged at 12,000 × *g* for 5 min. A 20 μL aliquot of the supernatant was used for identification of metabolites.

3. Results and discussion

3.1. Proposed CID pathway of the parent drug PAC-1

As metabolites often contain product ions related to those of parent compound, the parent compound's fragmentation behavior was first studied by LC-ITMS to characterize these structures. As indicated in Fig. 1, the protonated parent molecule showed *m/z*

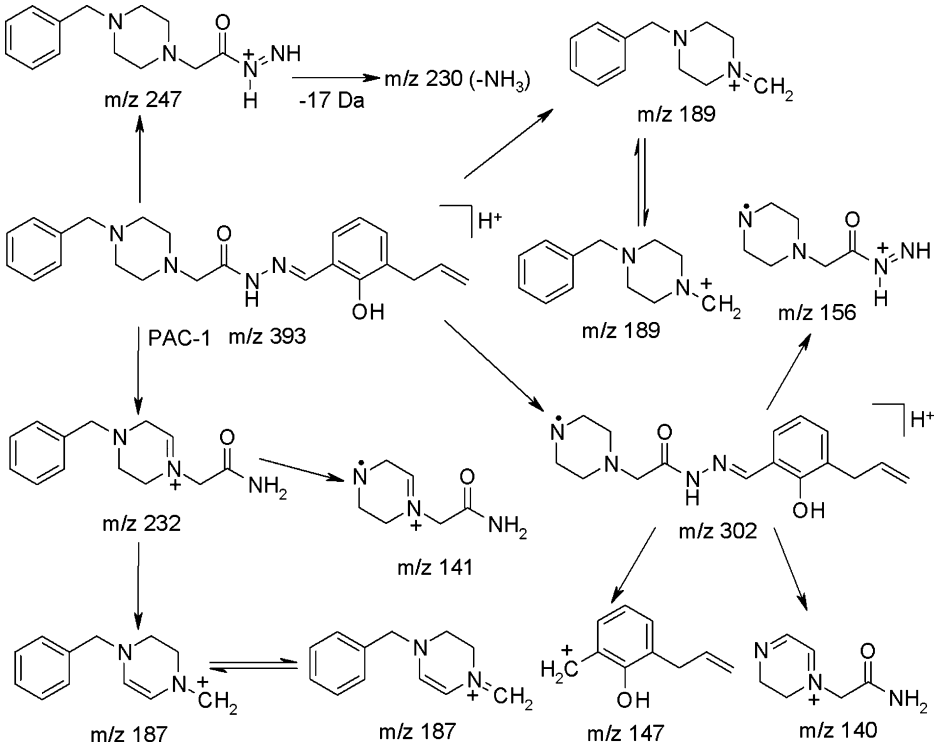

Fig. 2. Proposed CID pathways of PAC-1 at the precursor of *m/z* 393.

393 (Fig. 1A) with a trace ion of $[M+Na]^+$ (*m/z* 415). The MS/MS spectrum of the ion at *m/z* 393 displayed ions at *m/z* 302, 247, 232, 189 and 141 (Fig. 1B). The ion at *m/z* 302 was formed by the loss of benzyl radical (−91 Da with a proton shift), while the 232 ion was formed by rearrangement after cleavage of the N–N bond (−161 Da with a proton shift). The ion at *m/z* 247 was formed by the loss of the 3-allyl-2-hydroxy-benzylidene moiety (−146 Da with a proton shift). The main 189 ion was formed by the loss of the 3-allyl-2-hydroxy-benzylidene and hydrazide moiety (−204 Da with a proton shift), while the 141 ion was formed by rearrangement after the loss a benzyl radical, hydrazide moiety, and the 3-allyl-2-hydroxy-benzylidene moiety (−252 Da with a proton shift). The MS^3 spectrum of the ion at *m/z* 302 (393 → 302) showed fragment ions of *m/z* 156, 147 and 140 (Fig. 1C). The MS^3 spectrum of ion at *m/z* 247 (393 → 247) showed fragment ions of *m/z* 230, 187 and 156 (Fig. 1D), while MS^3 spectrum of the ion at *m/z* 232 (393 → 232) showed fragment ions of *m/z* 230, 187 and 141 (Fig. 1E).

Based on the above data, a CID pathway of the PAC-1 was proposed (Fig. 2). These ions were subsequently used as diagnostic product ions for identification of unknown metabolites through comparison of changes in observed mass (Δm) and mass spectral patterns of product ions with those of PAC-1.

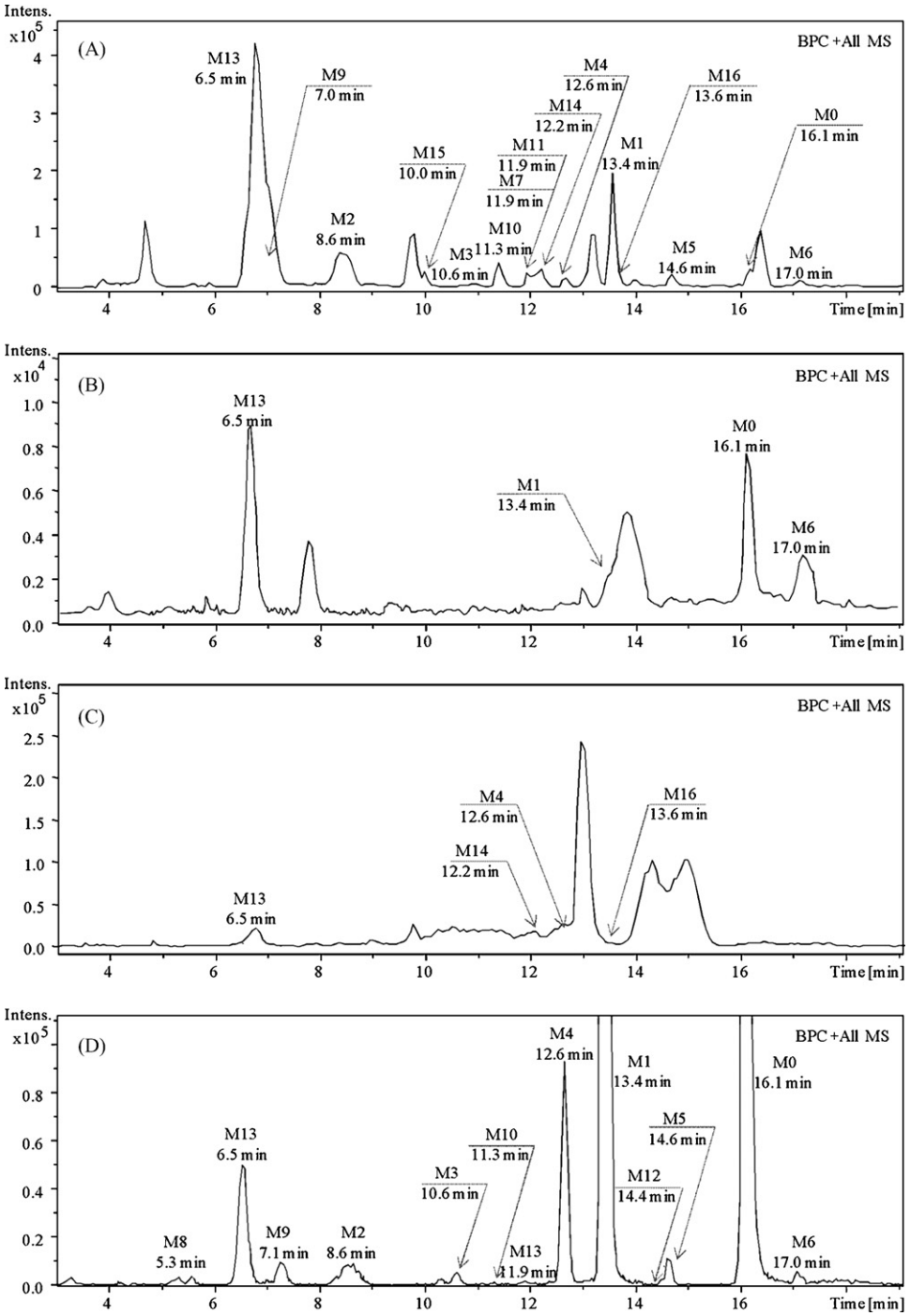

Fig. 3. Base peak chromatogram and profiling of PAC-1 and metabolites (A) urine sample, (B) feces sample, (C) bile sample and (D) *in vitro* sample.

3.2. Identification of the metabolites

In vivo and *in vitro* samples were first screened for metabolites using a LC-Q-TOF/MS system, and exact mass data were obtained for all detected compounds. Careful mining of the data collected from the LC-Q-TOF/MS system resulted in the discovery of 16 metabolites in rat urine, feces, bile, and *in vitro* samples. All metabolites were also detected in a later analysis on the LC-ITMS system for structure elucidation. The base peak chromatograms of all *in vivo* and *in vitro* detected metabolites are shown in Fig. 3. These metabolites are also listed in Table 1 along with measured mass-to-charge ratios (*m/z*), calculated mass-to-charge ratios (*m/z*), protonated molecule formulas, mass accuracy, retention times, and MS^n data.

3.2.1. M0

The LC retention time of the PAC-1 standard was 16.1 min. Therefore, a peak at 16.1 min with a protonated ion at *m/z* 393 indicated non-metabolized PAC-1. However, a peak at 12.2 min with *m/z* 393 was also observed from the rat urine sample. Analysis indicated that this peak was the result of the in-source CID from the PAC-1 glucuronide conjugate (*M14*). It was important to be aware of the existence of these glucuronide conjugates as well as their related free forms so that ions from the in-source CID were not assigned as new metabolites.

3.2.2. M1

Found in rat urine, feces and RLM samples, *M1* was observed at a retention time of 13.4 min with a protonated ion at *m/z* 303 (*m/z* 393–90 Da). The MS/MS spectrum at *m/z* 303 displayed major product ions at *m/z* 286 (−17 Da, loss of NH_3), 203, 177 and 147. Apparently, the protonated ion of *M1* was 90 Da less than that of PAC-1, suggesting that this metabolite was debenzylated PAC-1. After comparison with the reference obtained from incubation using RLM supplemented with NADPH, *M1* was positively identified as des-benzyl-PAC-1.

3.2.3. M2–M6

The five metabolites, *M2–M6*, appeared to be odd-oxygen added products since their $[M+H]^+$ ions were all at *m/z* 409 (*m/z* 393 + 16 Da) with the retention times at 8.6, 10.6, 12.6, 14.6 and 17.0 min, respectively. *M2–M6* were found in rat urine and RLM samples. In addition, *M4* was also found in rat bile samples and *M6* was also found in rat feces samples.

The MS/MS spectra of *M2* and *M4* displayed nearly identical ions: *m/z* 391 (−18 Da, loss of H_2O), 318 (−91 Da, loss of benzyl radical), 232, 189 and 141. The ions at *m/z* 232, 189 and 141, the same as those of PAC-1, suggested that the 4-benzyl-piperazin-1-yl moiety was not metabolically modified. Furthermore, the MS^3 spectra of *M2* and *M4* (409 → 318) showed fragment ions of *m/z* 259, 163 and 140. The ion at *m/z* 163, 16 Da higher than that of PAC-1 (*m/z* 147), supported the notion that hydroxylation occurred at the 3-allyl-2-hydroxy-benzylidene moiety.

The MS/MS spectrum of *M3* displayed ions at *m/z* 391 and 189. The ion at *m/z* 391 (−18 Da, loss of H_2O), indicated hydroxylation had occurred. Further, the MS^3 spectrum of *M3* (409 → 391) showed fragment ions of *m/z* 300, 232, 189 and 141, the same as those of PAC-1, suggesting that the 4-benzyl-piperazin-1-yl moiety was not metabolically modified. Thus, *M3* was likely a monohydroxylated product of PAC-1, with oxidation taking place at the 3-allyl-2-hydroxy-benzylidene moiety.

The MS/MS spectrum of *M5* displayed ions at *m/z* 391, 303 and 249. The product ions at *m/z* 391 (−18 Da, loss of H_2O) and 303 (−90–16 Da, loss of benzyl and hydroxyl moieties), suggesting *M5* was a hydroxylated product of PAC-1, with oxidation taking place on the benzyl moiety.

Table 1
Metabolites identified in biological samples using LC-ESI-Q-TOF/MS and LC-ESI-ITMS.

	m/z	Measured $[M+H]^+$	Calculated $[M+H]^+$	Formula	Error (ppm)	RT (min)	MS/MS fragments	MS^3 fragments
M0	393	393.2283	393.2285	$C_{23}H_{29}N_4O_2$	0.6	16.1	MS/MS/393: 302, 247, 232, 189 (100%), 141	MS^3/302: 156, 140 (100%), 147 MS^3/232: 230, 187, 141 (100%)
M1	303	303.1818	303.1816	$C_{16}H_{23}N_4O_2$	−0.8	13.4	MS/MS/303: 286, 203, 177, 157, 147 (100%), 142	
M2	409	409.2232	409.2234	$C_{23}H_{29}N_4O_3$	0.5	8.6	MS/MS/409: 391, 318 (100%), 232, 189, 163, 141	MS^3/318: 288, 259, 178, 163, 140 (100%)
M3	409	409.2229	409.2234	$C_{23}H_{29}N_4O_3$	1.2	10.6	MS/MS/409: 391 (100%), 189	MS^3/391: 300, 232, 189 (100%), 141
M4	409	409.2228	409.2234	$C_{23}H_{29}N_4O_3$	1.5	12.6	MS/MS/409: 391, 318, 232, 189 (100%), 141	MS^3/318: 259, 163, 140 (100%)
M5	409	409.2214	409.2234	$C_{23}H_{29}N_4O_3$	4.9	14.6	MS/MS/409: 391, 303 (100%), 249	MS^3/303: 217, 203, 177, 147 (100%)
M6	409	409.2222	409.2234	$C_{23}H_{29}N_4O_3$	3.3	17.0	MS/MS/409: 391, 300 (100%), 260, 219, 189, 162	
M7	423	423.2029	423.2027	$C_{23}H_{27}N_4O_4$	−0.5	11.9	MS/MS/423: 405, 379 (100%), 232, 189	MS^3/379: 288, 232, 247, 189 (100%), 141
M8	425	425.2150	425.2183	$C_{23}H_{29}N_4O_4$	7.8	5.3	MS/MS/425: 407, 334, 286, 232, 189 (100%), 141	
M9	425	425.2169	425.2183	$C_{23}H_{29}N_4O_4$	3.1	7.1	MS/MS/425: 407, 334 (100%), 251, 232, 189, 141	
M10	425	425.2159	425.2183	$C_{23}H_{29}N_4O_4$	−5.7	11.3	MS/MS/425: 319 (100%)	MS^3/319: 233, 219, 193, 163 (100%), 142
M11	425	425.2163	425.2183	$C_{23}H_{29}N_4O_4$	4.9	11.9	MS/MS/425: 407, 334, 232, 189 (100%), 141	MS^3/334: 317, 275, 179, 156 (100%), 140
M12	425	425.2208	425.2183	$C_{23}H_{29}N_4O_4$	−5.7	14.5	MS/MS/425: 303 (100%)	MS^3/303: 286, 217, 203, 177, 147 (100%)
M13	427	427.2329	427.2340	$C_{23}H_{31}N_4O_4$	2.5	6.5	MS/MS/427: 409, 336, 232, 189 (100%), 141	MS^3/336: 319, 277, 263, 181, 156, 140 (100%)
M14	569	569.2616	569.2606	$C_{29}H_{37}N_4O_8$	−1.7	12.2	MS/MS/569: 393 (100%), 189	MS^3/393: 302, 232, 189, 141 (100%)
M15	585	585.2549	585.2555	$C_{29}H_{37}N_4O_9$	1.0	10.0	MS/MS/585: 409, 318, 277, 189 (100%)	
M16	585	585.2548	585.2555	$C_{29}H_{37}N_4O_9$	1.1	13.6	MS/MS/585: 409, 303, 203, 107 (100%)	

The MS/MS spectrum of *M6* displayed ions at *m/z* 391, 300, 219 and 189. The ion at *m/z* 391 (−18 Da, loss of H_2O), indicated hydroxylation had occurred. The ion at *m/z* 219, 16 Da higher than *m/z* 203 which appears in the MS/MS spectrum of *M1*, indicated hydroxylation had occurred at the 3-allyl-2-hydroxy-benzylidene moiety.

3.2.4. M7

Found in rat urine samples, *M7* was observed at retention times of 11.9 min with a protonated ion at *m/z* 423 (*m/z* 393 + 30 Da).

The MS/MS spectrum of *M7* displayed ions at *m/z* 405, 379, 247, 232 and 189. The ions at *m/z* 232 and 189, the same as those of PAC-1, suggested that modification did not occur at the 4-benzyl-piperazin-1-yl moiety. Rather, the ions at *m/z* 405 (−18 Da, loss of H_2O) and *m/z* 379 (−44 Da, loss of CO_2) strongly suggested that a carboxyl group had been incorporated into the metabolite. The MS^3 spectrum of *M7* (423 → 379) showed fragment ions of *m/z* 288 (−91 Da, loss of benzyl radical from the ion at *m/z* 379), 247, 232, 189 and 141, indicating that this carboxyl group was located at the 3-allyl moiety, after structural rearrangement. Therefore, *M7* was tentatively assigned as carboxylated PAC-1.

3.2.5. M8–M12

With protonated ions at *m/z* 425 (*m/z* 393 + 32 Da), *M8–M12* were observed at retention times of 5.3, 7.1, 11.3, 11.9, and 14.5 min, respectively. The five metabolites, *M8–M12*, were found in RLM samples. In addition, *M9*, *M10* and *M11* were also found in rat urine samples.

The MS/MS spectra of *M8*, *M9* and *M11* displayed nearly identical ions: *m/z* 407, 334, 232, 189 and 141. The ions at *m/z* 232, 189 and 141, the same as those of PAC-1, suggested that modification did not occur at the 4-benzyl-piperazin-1-yl moiety. The ions at *m/z* 407 (−18 Da, loss of H_2O) and 334 (−91 Da, loss of benzyl) were both 16 Da higher than corresponding ions at *m/z* 391 and 318 in the MS/MS spectrum of mono-hydroxylated PAC-1(*M2* and *M4)*, suggesting that *M8*, *M9 and M11* could be dihydroxylation products of PAC-1.

The MS/MS spectrum of *M10* displayed only one ion at *m/z* 319. The ion at *m/z* 319 (−90–16 Da, loss of benzyl radical and hydroxyl group), indicated that there was a hydroxyl group on the benzyl moiety. Further, the MS^3 spectrum of *M10* (425 → 319) showed fragment ions of *m/z* 219, 163 and 142. The ion at *m/z* 163 was 16 Da higher than *m/z* 147 which appears in the MS^3 spectrum of PAC-1 (393 → 302), suggesting that there was an additional hydroxyl group at the 3-allyl-2-hydroxy-benzylidene moiety. Thus, *M10* was tentatively identified as a dihydroxylation product of PAC-1.

The MS/MS spectrum of *M12* displayed one ion at *m/z* 303 (−90–32 Da, loss of benzyl radical and two hydroxyl groups). The MS^3 spectrum of the *M12* (425 → 303) showed fragment ions of *m/z* 286, 217, 203, 177 and 147, which were identical to the ions observed in the MS/MS spectrum of *M5*. This indicated that there were two hydroxyl groups added on benzyl moiety. Hence, *M12* was a further hydroxylated metabolite of *M5*.

3.2.6. M13

Found in rat urine, feces, bile and RLM samples, *M13* was observed at a retention time of 6.5 min with a protonated ion at *m/z* 427 (*m/z* 393 + 34 Da). The MS/MS spectrum of *m/z* 427 displayed ions at *m/z* 336 (−91 Da, loss of benzyl radical), 232, 189 and 141. The ions at *m/z* 232, 189 and 141, the same as those of PAC-1, suggested that modification did not occur at the 4-benzyl-piperazin-1-yl moiety. Furthermore, the MS^3 spectrum of the *M13* (427 → 336) showed fragment ions at *m/z* 319, 181, 156 and 140. The ion at *m/z* 181, 34 Da higher than that of *m/z* 147, suggested modification had only occurred at the 3-allyl moiety. Therefore, *M13* was tentatively identified as a dihydrodiol formation product of PAC-1.

Table 2
Metabolites of PAC-1 detected in rat.

	m/z	Identification	Biological matrices			
			RLM	Urine	Feces	Bile
M0	393	PAC-1	+	+	+	–
M1	303	PAC-1 − C_7H_6	+	+	+	(
M2	409	PAC-1 + O	+	+	(	(
M3	409	PAC-1 + O	+	+	(	(
M4	409	PAC-1 + O	+	+	(	+
M5	409	PAC-1 + O	+	+	(	(
M6	409	PAC-1 + O	+	+	+	(
M7	423	PAC-1 − H_2 + O_2	(	+	(	(
M8	425	PAC-1 + 2O	+	(	(	(
M9	425	PAC-1 + 2O	+	+	(	(
M10	425	PAC-1 + 2O	+	+	(	(
M11	425	PAC-1 + 2O	+	+	(	(
M12	425	PAC-1 + 2O	+	(	(	(
M13	427	PAC-1 + H_2O_2	+	+	+	+
M14	569	PAC-1 + Glu	(	+	(	+
M15	585	PAC-1 + O + Glu	(	+	(	(
M16	585	PAC-1 + O + Glu	(	+	(	+

3.2.7. M14

Found in rat urine and bile samples, *M14* was observed at a retention time of 12.2 min with a protonated ion at *m/z* 569 (*m/z* 393 + 176 Da). The neutral loss of 176 Da was observed from MS/MS spectra of *M14*. Furthermore, the MS^3 spectrum of the *M14* (569 → 393) showed fragment ions at *m/z* 302, 232, 189 and 141, which identical to those ions displayed in the MS/MS spectrum of PAC-1, suggesting that *M14* was a glucuronide conjugate of PAC-1.

3.2.8. M15 and M16

M15 and *M16* were observed at retention times of 10.0 min and 13.6 min, respectively, with the same $[M+H]^+$ ions at *m/z* 585 (*m/z* 393 + 16 Da + 176 Da). *M15* was only found in rat urine samples, and *M16* was found in rat urine and bile samples. The neutral loss of 176 Da was also observed from the MS/MS spectra of *M15* and *M16*, suggesting that both were glucuronide conjugates of hydroxylated PAC-1. The MS/MS spectrum of the *m/z* 585 (*M15*) showed fragment ions at *m/z* 409, 318 and 189. The ion at *m/z* 318, 16 Da higher than that of *m/z* 302, suggested hydroxylation had occurred at the 3-allyl-2-hydroxy-benzylidene moiety. The MS/MS spectrum of the *m/z* 585 (*M16*) showed fragment ions at *m/z* 409, 303 and 203. The ion at *m/z* 303 (*m/z* 585–176–90–16 Da), suggested hydroxylation had occurred on the benzyl moiety.

The LC-TOF/MS is becoming a more well-established tool in DMPK research, as it has the ability to perform exact mass measurements, resulting in the identification of elemental compositions of unknown metabolites. The combination of LC-Q-TOF/MS and LC-ITMS enabled us to profile the biotransformation of PAC-1. As a result, the metabolic information presented above is collectively presented in Table 2, and the proposed metabolic pathways of PAC-1 in rat are shown in Fig. 4.

PAC-1 had a fragmentation pattern as a result of homolytic bond cleavage in the MS/MS spectrum due to the benzyl moiety. This cleavage would form an odd-electron ion with the loss of benzyl radical, which then sequentially lost of neutral groups in the MS^3 spectrum. This fragmentation sequence was also observed from most metabolites, which could be used to identify whether metabolites were modified on benzyl moiety or not.

An additional issue that should be taken into consideration was the in-source collision. A good example from the present work is the in-source fragment ions from phase II conjugates. Otherwise,

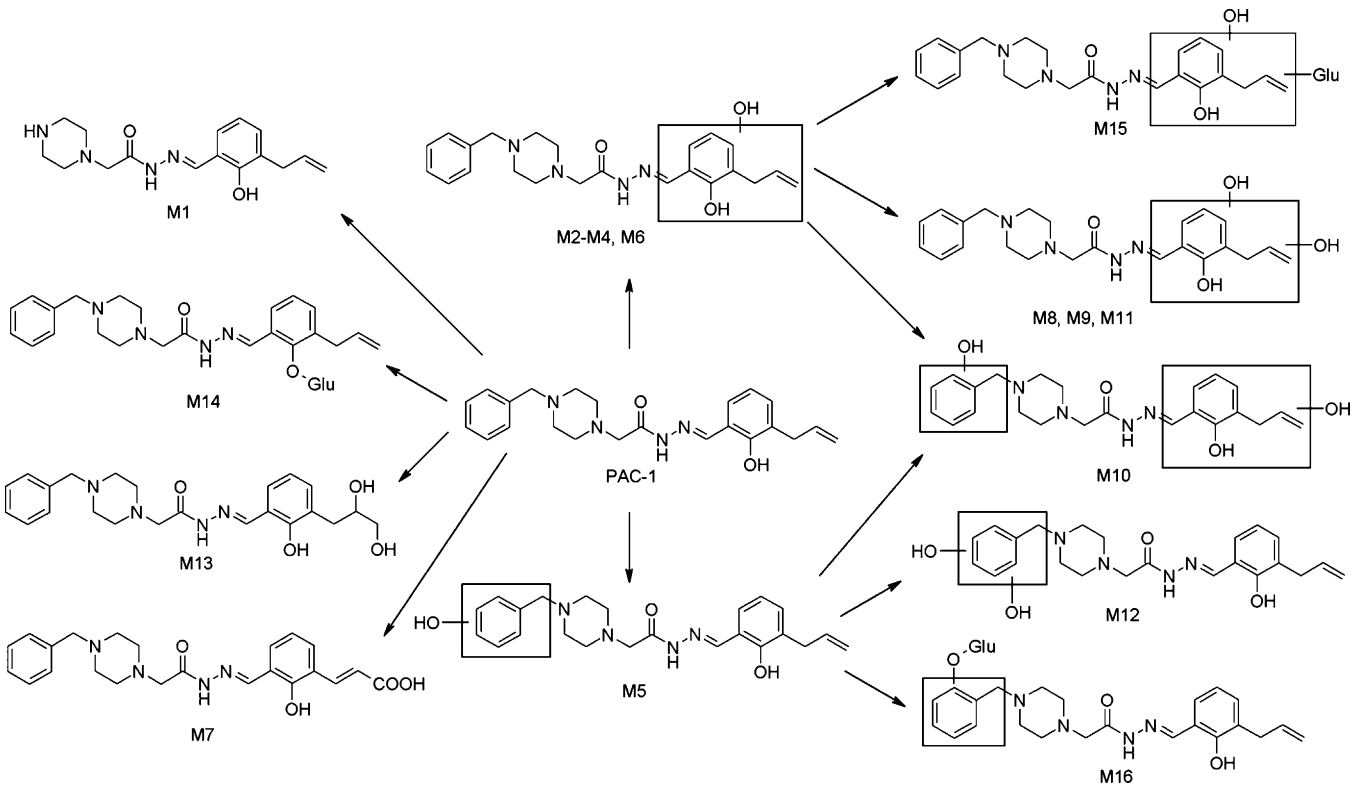

Fig. 4. Proposed major metabolic pathways of PAC-1 in rat.

it is readily possible that some metabolites could be identified are false positives.

The present study has demonstrated that PAC-1 has diversified and important metabolic pathways. There are altogether 16 metabolites including 13 phase I metabolites and 3 phase II metabolites detected and identified for the first time. Major metabolites identified are *M1* and *M13*. Formation of these metabolites can be explained by four proposed pathways: (1) the debenzylation (*M1*), (2) the hydroxylation and dihydroxylation (*M2–M6*, *M8–M12*), (3) the carboxylation (*M7*) and dihydrodiol formation (*M13*), and (4) the glucuronide conjugation (*M14–M16*). Most metabolites are detected in urine and RLM samples, while only a few trace level metabolites are found in bile and feces samples.

4. Conclusions

In summary, the profiling of the biotransformation of PAC-1 *in vivo* and *in vitro* has been carried out by LC-Q-TOF/MS and LC-ITMS. The combination of the structural information provided by the product ion spectra measurements with information on the elemental compositions of the metabolites provided by accurate mass determinations enable us to characterize the metabolites of PAC-1 and to propose its metabolic pathways in rat. This important metabolic data serve as a useful resource to support further studies of PAC-1. However, the role of cytochrome P450 in the biotransformation of PAC-1 is still under further study in our laboratory.

References

[1] N.J. Clarke, D. Rindgen, W.A. Korfmacher, K.A. Cox, Anal. Chem. 15 (2001) 430A.
[2] A.E. Nassar, R.E. Talaat, A.M. Kamel, Curr. Opin. Drug Discov. Devel. 9 (2006) 61.
[3] E.J. Oliveira, D.G. Watson, Biomed. Chromatogr. 6 (2000) 351.
[4] K.S. Putt, G.W. Chen, J.M. Pearson, J.S. Sandhorst, M.S. Hoagland, J.T. Kwon, S.K. Hwang, H. Jin, M.I. Churchwell, M.H. Cho, D.R. Doerge, W.G. Helferich, P.J. Hergenrother, Nat. Chem. Biol. 2 (2006) 543.
[5] J.B. Denault, M. Drag, G.S. Salvesen, J. Alves, A.B. Heidt, Q. Deveraux, J.L. Harris, Nat. Chem. Biol. 3 (2007) 519, author reply 520.
[6] A.G. Porter, Nat. Chem. Biol. 2 (2006) 509.
[7] S. Seton-Rogers, Nat. Rev. Drug Discov. 5 (2006) 818.
[8] S. Seton-Rogers, Nat. Rev. Cancer 6 (2006) 748.
[9] P. Kovacic, J. Recept Signal Transduct Res. 28 (2008) 141.
[10] S.A. Chan, M.J. Chen, T.Y. Liu, M.R. Fuh, J.F. Deng, M.L. Wu, S.J. Hsieh, Talanta 60 (2003) 679.
[11] W. Lam, R. Ramanatyhan, J. Am. Soc. Mass Spectrom 13 (2002) 345.
[12] B.Y. Ge, H.X. Chen, F.M. Han, Y. Chen, J. Chromatogr. B: Biomed. Sci. Appl. 857 (2007) 281.
[13] F.M. Han, Z.H. Peng, W. Song, g H.M. Zhan, M.M. Zhu, Y. Chen, J. Chromatogr. B: Biomed. Sci. Appl. 854 (2007) 1.
[14] M. Jemal, Z. Ouyang, W. Zhao, M. Zhu, W.W. Wu, Rapid. Commun. Mass Spectrom 17 (2003) 2732.
[15] L. Ernster, P. Siekevitz, G.E. Palade, J. Cell Biol. 15 (1962) 541.
[16] M. Markwell, S.M. Haas, L.L. Bieber, N.E. Tolbert, Anal. Biochem. 87 (1978) 210.
[17] T. Omura, R. Sato, J. Biol. Chem. 239 (1964) 2370.